

## Accepted Manuscript

Title: The impact of body fat on three dimensional motion of the paediatric foot during walking

Author: Ryan Mahaffey Stewart C. Morrison Paul Bassett  
Wendy I. Drechsler Mary C. Cramp



PII: S0966-6362(15)00977-7  
DOI: <http://dx.doi.org/doi:10.1016/j.gaitpost.2015.12.009>  
Reference: GAIPOS 4642

To appear in: *Gait & Posture*

Received date: 27-11-2014  
Revised date: 24-8-2015  
Accepted date: 3-12-2015

Please cite this article as: Mahaffey R, Morrison SC, Bassett P, Drechsler WI, Cramp MC, The impact of body fat on three dimensional motion of the paediatric foot during walking, *Gait and Posture* (2015), <http://dx.doi.org/10.1016/j.gaitpost.2015.12.009>

This is a PDF file of an unedited manuscript that has been accepted for publication. As a service to our customers we are providing this early version of the manuscript. The manuscript will undergo copyediting, typesetting, and review of the resulting proof before it is published in its final form. Please note that during the production process errors may be discovered which could affect the content, and all legal disclaimers that apply to the journal pertain.

### Highlights

- We explored potential relationships between foot segment motion and body fat in boys
- Higher fat mass predicted greater calcaneal plantarflexion in early and late stance and late swing
- Greater calcaneal abduction throughout stance and swing was predicted by higher fat mass
- Higher fat mass predicted greater midfoot dorsiflexion and eversion throughout the gait cycle
- Findings indicate a pronated foot type in boys with higher fat mass

**Title page****Title**

The impact of body fat on three dimensional motion of the paediatric foot during walking.

**Keywords**

Paediatric obesity, gait analysis, foot kinematics, 3D motion capture, multivariate analysis

**Authors**

Ryan Mahaffey<sup>1\*</sup>

\* Corresponding author

Email: [r.mahaffey@uel.ac.uk](mailto:r.mahaffey@uel.ac.uk)

Tel: +44 (0)20 8223 4110

Stewart C Morrison<sup>1</sup>

Email: [S.C.Morrison@uel.ac.uk](mailto:S.C.Morrison@uel.ac.uk)

Paul Bassett<sup>2</sup>

Email: [paul@statsconsultancy.co.uk](mailto:paul@statsconsultancy.co.uk)

Wendy I Drechsler<sup>1</sup>

Email: [W.Drechsler@uel.ac.uk](mailto:W.Drechsler@uel.ac.uk)

Mary C Cramp<sup>3</sup>

Email: [Mary.Cramp@uwe.ac.uk](mailto:Mary.Cramp@uwe.ac.uk)

<sup>1</sup> School of Health, Sport and Bioscience, University of East London, Stratford, London E15 4LZ, England

<sup>2</sup> Statsconsultancy Ltd. 40 Longwood Lane, Amersham, Bucks, HP7 9EN, England

<sup>3</sup> Department of Allied Health Professions, Glenside Campus, University of West England, Blackberry Hill, Bristol BS16 1DD, England

## 1. Introduction

Childhood obesity is associated with significant comorbidity and disability [1]. Worldwide prevalence of childhood overweight and obesity increased from 4.2% in 1990 to 6.7% in 2010 and is expected to reach 9.1% in 2020 [2]. Recent data from the UK National Child Measurement Programme estimated rates of overweight and obesity in England at 29% and 15% respectively [3]. Childhood obesity is associated with reduced physical activity and engagement in childhood activities [4], along with multiple health co-morbidities [5]. Childhood obesity has been reported to impact on the functional characteristics of the lower limb, potentially predisposing children to pain and discomfort during gait and musculoskeletal comorbidities [6]. Recent studies have reported reduced hip and knee flexion during gait and greater valgus positioning of the knee [7]. These findings support the view that obesity predisposes joint dysfunction and underpins a theoretical association with musculoskeletal pathology. Despite this, few studies have documented the impact of childhood obesity on the foot. Given the distal location and flexibility of the paediatric foot there is an increased susceptibility to pathology and deformation. It follows that any external influence upon the developing foot, such as obesity, may affect its function during gait [8].

Research on the plantar loading profiles of the paediatric foot have demonstrated childhood obesity to increase peak vertical forces [9], increase plantar contact area [10] and elevate plantar pressures [11] under the medial longitudinal arch. Emerging from this is the view that childhood obesity is associated with a pes planus foot type which, coupled with altered joint function, may predispose to the development of foot discomfort and pathologies [9,10,11]. Recent work supports the association between obesity and structural foot changes but given plantar pressure analysis is limited to two-dimensional analysis of the foot during stance more work is required to characterise the impact of childhood obesity on the three-dimensional foot during the gait cycle. A recent study looking at the kinematics of sagittal and frontal plane lower limb motion in overweight boys [12] reported greater rear-foot eversion during gait. This finding supports the view of pes planus and a pronated foot type and suggests that obesity affects the function of the paediatric foot during walking. However, the findings are limited as this work did not take into account the complex motion of the multiple foot segments. Determining the intersegmental motion of the foot during gait can help to inform current approaches to rehabilitation and underpin clinical interventions where foot and joint problems in childhood obesity are indicated. The aim of this study was to explore the relationships between intersegmental foot motion during gait and obesity (measured by body fat) in boys between the age of 7 and 11 years. It was hypothesised that body fat (obesity

level) would be associated with altered intersegment foot motion over the gait cycle, particularly in the midfoot.

## 2. Methods

### 2.1. Selection and Description of Participants

Fifty-five boys, aged seven to eleven years, participated in the study and participant characteristics are presented in Table 1. Ethical approval was obtained from the host institution (Ref No. ETH/13/11) and parental consent was obtained prior to testing. All participants were recruited from local school children. Exclusion criteria included medical conditions affecting neuromuscular and orthopaedic integrity or any complications contributing to altered foot posture and/or gait disturbance.

### 2.2. Instrumentation and Procedures

#### 2.2.1. Measures of Anthropometrics and Body fat

Body fat (level of obesity) was measured by air displacement plethysmography using a Bodpod (Life Measurement, Inc, Concord, CA, USA). Estimates of body volume were derived from pressure measures within the Bodpod chamber under isothermal and adiabatic conditions [13]. The Bodpod has been shown to be a reliable and accurate measure of body fat in healthy and obese children [14, 15]. Each participant wore swimming shorts and a swimming cap and was asked to enter the Bodpod chamber and remain still for 40 seconds for three successive trials. Changes in pressure were measured and averaged across the three trials to calculate body volume. Raw body volumes were corrected for isothermal air in the lungs and close to the skin surface using child-specific equations [16, 17]. Corrected body volumes were converted to body percentages using age- and gender- specific equations [18]. Body fat was expressed as percentage fat mass relative to total body mass. Weight was measured to the nearest 0.1 kg using Bodpod scales and height measured to the nearest 0.5 cm using a portable Leicester stadiometer (Seca Leicester portable stadiometer; Seca Vogel, Hamburg, Germany). Body Mass Index (BMI) score was calculated as  $\text{height}/\text{weight}^2$  and reported as an age and sex specific z-score (standard deviation score). This was based on the distribution of BMI in the UK90 growth reference [19] using a Microsoft Excel macro developed for use with this growth reference (Child Growth Foundation, Chiswick, UK).

## 2.2.2. Measures of spatiotemporal and 3D intersegment foot motion during gait

An eight-camera Vicon Nexus motion capture system (Vicon Motion Systems Ltd, Oxford, UK) was used to track and record the motion of skin mounted reflective markers at 200Hz during barefoot walking at self-selected speed. Fifteen 9mm retro-reflective markers were attached to the right shank and foot of each participant in line with the 3DFoot model [20]. Previous research has demonstrated the reliability of this foot model in a paediatric population [21]. A four segment model of the foot was constructed for calculation of relative intersegment angular motion in Visual 3D software (C-Motion Inc., MD, USA). Two floor mounted force plates (Bertec, Model MIE Ltd, Leeds, UK) recorded ground reaction forces during gait trials at 1000 Hz. The gait cycle was defined from initial contact (determined as an increase in vertical force ( $F_z$ ) above 20N) through foot-off and the subsequent initial contact of the same foot. Sagittal, frontal and transverse planar motion was described for the shank-calcaneus, calcaneus-midfoot and midfoot-metatarsals segments of the right foot. 3D intersegment foot angles from each participant were extracted as 51 data points normalised over the gait cycle representing angular waveform patterns of foot segment motion. Mean 3D intersegment angles were calculated for each participant based on ten gait cycles captured.

## 2.3. Statistical analysis

### 2.3.1. Principal Component Analysis (PCA)

Principle component analysis (PCA) was employed to reduce the major modes of variation in the data in order to fully explore foot segment motion over the entire gait cycle. Previous research on paediatric gait has employed PCA to analyse multiple waveforms utilising separate matrices [22]). In the current study, nine matrices (3 segmental angles of shank-calcaneus, calcaneus-midfoot, midfoot-metatarsals each in 3 planes of sagittal, frontal and transverse) were constructed for 3D foot angle waveforms based on the 55 participants and the 51 points (55 x 51). The features of variation in the waveform data were extracted using PCA by orthogonally rotating the variables, using a varimax method, into components which maximally explained variability in the original waveforms. Principal components (PC) were retained that cumulatively explained at least 90% of the waveform variation. The rotated loadings (describing the proportion of variance explained by the underlying data points) were assessed to determine which data points contributed to each component. Rotated loadings in excess of 0.722 or below -0.722 were considered as contributing to

a component [24]. A regression score (estimated coefficient representing a participants score on a component) of was calculated for each participant based on their 3D intersegment foot angle within each PC. Positive regression scores indicated dorsiflexion, eversion and abduction and negative regression scores indicated plantarflexion, inversion and adduction. This regression score was used for subsequent analysis by multiple linear regression analysis.

### 2.3.2. Multiple linear regression

In order to determine the association between body fat and 3D intersegment foot angles, the regression scores extracted from PCA were entered into multiple linear regression. The regression score was entered as the dependent variable and obesity as the predictor variable. Based on the potential confounding effects which may influence the relationship between obesity and 3D intersegment foot motion, eight potential confounding predictor variables (age, height, BMI Z-Score, walking speed, step length, step width, stance phase duration and total single support phase duration) were entered into multiple linear regression. To account for the possibility of a curvilinear relationship between the predictor variables and the regression score, a second order polynomial (e.g.  $\text{body fat}_{\text{quad}}$ ) was fitted to each predictor variable. The linear (e.g.  $\text{body fat}_{\text{lin}}$ ) and curvilinear (e.g.  $\text{body fat}_{\text{quad}}$ ) predictor variables were entered into multiple linear regression. For the exploratory nature of the study a backward step-wise regression method was used to determine the predictors for the regression scores based on 3D intersegment foot motion. Predictor variables were removed in the order of least significance (i.e. highest  $p$  value) until the remaining predictors (if any), were significantly associated with the regression score. If obesity and one or more other variables were significantly associated with the regression score, further analysis in mixed model linear regression to account for the potentially confounding influence amongst the predictor variables was undertaken. Only those regression scores that were significantly associated with obesity are presented in the results. All statistical analysis was carried out in SPSS version 20. Statistical significance was set to  $p < .05$ .

## 3. Results

### 3.1. Demographic, anthropometric and spatiotemporal characteristics of the participants

Table 1 shows the demographic, anthropometric and spatiotemporal characteristics of the participants. According to the UK90 BMI Z-Score cut-offs for children [19], 8 participants were

classified as obese, 12 participants were classified overweight, 29 as ideal weight and 6 were underweight.

### 3.2. Principal Component Analysis

Table 2 presents the results of PCA of the three foot joints, each joint in three planes of motion. Four shank-calcaneus sagittal plane angular PC were extracted from the original waveform, explaining 97.62% of the variance (Figure 1 *a, e*). Two shank-calcaneus frontal plane PCs were extracted from the original waveform, explaining 95.47% of the variance. Two shank-calcaneus transverse plane PCs were extracted from the original waveform, explaining 96.79% of the variance (Figure 1 *b, f*).

One calcaneus-midfoot sagittal plane angular PC was extracted from the original waveform, explaining 96.56% of the variance in angular motion (Figure 1 *c, g*). Calcaneus-midfoot frontal plane waveform was captured in one PC, explaining 97.39% of the variance (Figure 1 *d, h*). One calcaneus-midfoot transverse plane angular PC was extracted, explaining 99.31% of the variance.

Two midfoot-metatarsal sagittal plane angular PCs were extracted from the original waveform, explaining 98.17% of the variance. One midfoot-metatarsal frontal plane angular PC was extracted explaining 96.97% of variance and one midfoot-metatarsal transverse plane angular PC was extracted covering 98.76% of the variance.

### 3.3. Multiple linear regression analysis

Significant findings from the regression analysis are presented in Table 3. A regression model containing body fat<sub>linear</sub> and stance phase duration<sub>linear</sub> was significant in predicting shank-calcaneus sagittal PC1. Mixed model regression confirmed the significant association between body fat<sub>linear</sub> and stance phase duration<sub>linear</sub> with PC1 ( $F=7.35, p=.009$  and  $F=23.71, p<.000$  for body fat<sub>linear</sub> and stance phase duration<sub>linear</sub> respectively). Higher obesity and greater stance phase duration were positively associated with plantarflexion of the calcaneus relative to the shank during the first half of the single support phase of the gait cycle. Body fat<sub>linear</sub> significantly predicted shank-calcaneus sagittal PC2 and PC3. Greater plantarflexion of the calcaneus relative to the shank during the end of stance (PC2) and the end of swing (PC3) was positively associated with higher.



A regression model containing body fat<sub>linear</sub> and body fat<sub>quad</sub> was significant in predicting shank-calcaneus transverse PC1. Mixed model regression confirmed the significant association between body fat<sub>linear</sub> and body fat<sub>quad</sub> with PC1 ( $F=3.18, p=.043$  and  $F=4.36, p=.026$ , for body fat<sub>linear</sub> and body fat<sub>quad</sub> respectively). Higher body fat was positively associated with greater abduction of the calcaneus relative to the shank through-out stance phase. Shank-calcaneus transverse plane motion, captured in PC2, was significantly predicted by body fat<sub>linear</sub>. Higher body fat was positively associated with greater abduction of the calcaneus relative to the shank through swing phase.

A regression model of body fat<sub>linear</sub> was significant in predicting calcaneus-midfoot sagittal PC1. Higher body fat was positively associated with greater dorsiflexion of the midfoot relative to the calcaneus throughout the gait cycle.

A regression model containing body fat<sub>linear</sub>, body fat<sub>quad</sub>, ZScore<sub>linear</sub>, Z-Score<sub>quad</sub>, Height<sub>linear</sub> and Step distance<sub>linear</sub> significantly predicted calcaneus-midfoot frontal PC1. Mixed model revealed a significant association between body fat<sub>linear</sub> ( $F=6.37, p=.026$ ), body fat<sub>quad</sub> ( $F=6.63, p=.017$ ), ZScore<sub>linear</sub> ( $F=10.86, p=.007$ ), Z-Score<sub>quad</sub> ( $F=14.51, p=.002$ ), Height<sub>linear</sub> ( $F=13.20, p=.003$ ) and Step distance<sub>linear</sub> ( $F=3.31, p=.041$ ) with PC1. Higher body fat and BMI Z-Score, greater height and longer step distance were positively associated with eversion of the midfoot relative to the calcaneus throughout the gait cycle.

Figure 2 summarises the significant relationships between body fat with shank-calcaneus and calcaneus-midfoot motion which indicates greater plantarflexion and adduction of the calcaneus and greater dorsiflexion and eversion of the midfoot during the gait cycle.

#### 4. Discussion

The aim of this study was to explore the relationships between intersegmental foot motion and body fat in a cohort of male participants. The findings offer novel relationships between angular motion between foot segments and body fat and support our hypothesis that body fat (obesity level) would be associated with altered angular motion of foot segments across the gait cycle, as illustrated in Figure 2.

The analysis of 3D shank-calcaneus motion demonstrated a relationship between higher body fat and greater calcaneus plantarflexion throughout the gait cycle. This finding concurs with McMillan

et al [7] who reported greater peak calcaneus plantarflexion during the early part of stance phase in obese compared to non-obese children. Greater plantarflexion of the calcaneus segment may represent a horizontal position of the calcaneal bone and a vertically orientated talus. This bone orientation has been previously reported in children with pes planus, indicating a lowering of the longitudinal arch and foot pronation [24].

Reduced shank-calcaneus adduction was identified in the participants with higher body fat across the whole gait cycle. Transverse plane analysis of obese/overweight children's feet have previously considered the foot as only one rigid segment [25]. Shultz et al., [25] reported reduced adduction, reported as external rotation, of the foot in overweight children compared to their healthy weight peers. Similar results were reported in an earlier study by Hills & Parker [26] which demonstrated greater external rotation of the foot, described by the authors as out-toeing, at all phases of the gait cycle. These authors proposed that greater out-toeing may encourage a wider base of support as a compensatory change to aid stability during walking. The results of the current study agree with previous reports of an externally rotated foot in obese children highlighting this rotation as occurring at the calcaneus relative to the shank

The current study also reported greater midfoot dorsiflexion throughout the gait cycle in boys with greater body fat. Adoracion Villarroya et al., [27] using radiographic imaging, found talus-first metatarsal sagittal plane angles in standing to be more dorsiflexed in obese children and adolescents compared to published normal values. The finding in this study of greater midfoot dorsiflexion is consistent with the view that obese children have a pronated foot-type. While comparisons between static foot alignments from radiographic measures may not compare directly with dynamic motion of the foot, both the calcaneus and midfoot sagittal plane orientation gives more evidence of a pronated foot [27].

Midfoot eversion found throughout the gait cycle in participants with higher body fat could also indicate a lowering of the medial longitudinal arch. This finding is consistent with previous studies evaluating dynamic plantar pressure in obese children. Mickle et al., [10] found higher peak pressures under the midfoot segment of obese children compared to their non-obese counterparts. Weakening or laxity of the arch supporting structures, due to excessive force incurred by the carriage of greater loads, may flatten the arch leading to the pronated foot-type [26]. These findings further support the view that obese children have a pronated foot during gait.

This study was limited in that the determination of predictor variables associated with intersegment foot motion was based on the findings from previous studies [26,29,30]. Although significant, the

predictor variables generally explained a low percentage of variance in intersegment foot motion. This finding suggests that other factors (e.g. foot type) may influence the relationship between body fat and foot segment motion. A second limitation was the use of multiple PCAs to examine variation in the foot kinematic data. Ideally a single PCA with all variables of interest should be run, however little data was available on which specific foot segments at certain points gait cycle to enter into the analysis. Therefore, PCA was utilised to reduce the total number of kinematic and temporal variables. Future research should focus on the specific foot segmental kinematics at certain points of the gait cycle. Furthermore, the findings from PCA demonstrated that several foot segment angular waveforms were considered as one component due to the small variation across the gait cycle versus variation between participants. These results suggest excessive body fat relates to a rotational offset in foot segment's structure rather than an alternative pattern of angular motion. Despite these limitations, this work offers novel data about the impact of obesity on the kinematics of the foot which may have impact of the rehabilitation strategies for children with obesity. Future studies should consider the relationships between measures of foot structure and function with obese children and if changes are associated with reduced pain, discomfort and decreased physical activity.

## **5. Conclusions**

This study presents novel information on the relationships between body fat and angular motion of foot segments during gait. The findings identified a more pronated foot type throughout the gait cycle in obese boys. The pronated foot type may have implications for the onset of pain and discomfort during weight bearing activities.

## **Acknowledgements**

Ryan Mahaffey was funded as a research assistant by the Dr William M. Scholl Podiatric Research and Development Fund.

## **Author contributions**

RM has contributed to the design of the study, the data collection and analysis, and the preparation of the manuscript

SM has contributed to the design of the study, and the preparation of the manuscript

PB has contributed to the statistical analysis, and the preparation of the manuscript

WD has contributed to the design of the study, and the preparation of the manuscript

MC has contributed to the design of the study, and the preparation of the manuscript

## Reference list

1. Tsiros MD, Coates AM, Howe PR, Grimshaw PN, Buckley JD. Obesity: the new childhood disability? *Obesity reviews: an official journal of the International Association for the Study of Obesity*. 2011;12(1):26-36.
2. de Onis M, Blössner M, Borghi E. Global prevalence and trends of overweight and obesity among preschool children. *The American journal of clinical nutrition*. 2010;92(5):1257-64.
3. National Child Measurement Program. (2014). National child measurement program (NCMP) 2013/14. <http://www.dh.gov.uk> Retrieved August 2014.
4. Shultz SP, Anner J, Hills AP Paediatric obesity, physical activity and the musculoskeletal system. *Obes Rev* 2009; 10/5: 576-82.
5. Ebbeling CB, Pawlak DB, Ludwig DS. Childhood obesity: Public-health crisis, common sense cure. *Lancet* 2002; 360 (9331): 473-82.
6. Shultz SP, Browning RC, Schutz Y, Maffei C, Hills AP. Childhood obesity and walking: guidelines and challenges. *International journal of pediatric obesity*. 2011;6(5-6):332-41.
7. McMillan AG, Pulver AM, Collier DN, Blaise Williams DS. Sagittal and frontal plane joint mechanics throughout the stance phase of walking in adolescents who are obese. *Gait Posture* 2010; 32(2): 263-8
8. Dawe EJC, Davis J. Anatomy and biomechanics of the foot and ankle. *Orthopaedics and Trauma* 2011; 25(4): 279-286
9. Cousins SD, Morrison SC, Drechsler WI. Foot loading patterns in normal weight, overweight and obese children aged 7 to 11 years. *J Foot Ankle Res* 2013; 6(1): 36
10. Mickle KJ, Steele JR, Munro BJ. Does excess mass affect plantar pressure in young children? *Int J Pediatr Obes* 2006; 1(3): 183-8
11. Song-hua, Y; Kuan, Z; Gou-qing, T; Jin, Y and Zhi-cheng, L. Effects of obesity of dynamic plantar pressure distribution in Chinese prepubescent children during walking. *Gait Posture* 2013; 32: 37-42.

12. McMillan AG, Auman NL, Collier DN, Blaise Williams DS. Frontal plane lower extremity biomechanics during walking in boys who are overweight versus healthy weight. *Pediatr Phys Ther* 2009; 21(2): 187-93
13. Dempster P, Aitkens S. A new air displacement method for the determination of human body composition. *Med Sci Sports Exerc* 1995; 27(12): 1692-7
14. Wells JC, Fuller NJ. Precision of measurement and body size in whole-body air-displacement plethysmography. *Int J Obes Relat Metab Disord* 2001; 25(8): 1161-7
15. Gately PJ, Radley D, Cooke CB, Carroll S, Oldroyd B, Truscott J G, et al. Comparison of body composition methods in overweight and obese children. *J Appl Physiol* 2003; 95(5): 2039-46
16. Haycock GB, Schwartz GJ, Wisotsky DH. Geometric method for measuring body surface area: A height-weight formula validated in infants, children, and adults. *J Pediatr* 1978; 93(1): 62-6
17. Fields DA, Hull HR, Cheline AJ, Yao M, Higgins PB. Child-specific thoracic gas volume prediction equations for air-displacement plethysmography. *Obes Res* 2004; 12(11): 1797-804
18. Lohman, TG. Assessment of body composition in children. *Ped Exerc Sci* 1989; 1: 19-30
19. Cole TJ, Freeman JV, Preece MA. Body mass index reference curves for the UK, 1990. *Arch Dis Child* 1995; 73(1): 25-9
20. Leardini A, Benedetti MG, Berti L, Bettinelli D, Nativo R, Giannini S. Rear-foot, mid-foot and fore-foot motion during the stance phase of gait. *Gait Posture* 2007; 25(3): 453-62
21. Mahaffey R, Morrison SC, Drechsler W, Cramp M. Evaluation of multi-segmental kinematic modelling in the paediatric foot using three concurrent foot models. *J Foot Ankle Res* 2013; 6: 43
22. Chester VL, Wrigley AT. The identification of age-related differences in kinetic gait parameters using principal component analysis. *Clinical Biomechanics* 2008; 23(2): 212-20.
23. Field A. *Discovering statistics using spss*. 3<sup>rd</sup> ed. London: Sage; 2009.
24. Kim HW, Weinstein SL. Flatfoot in children: Differential diagnosis and management. *Curr Orthop* 2000; 14(6): 441-7
25. Shultz SP, Sitler MR, Tierney RT, Hillstrom HJ, Song J. Effects of pediatric obesity on joint kinematics and kinetics during 2 walking cadences. *Arch Phys Med Rehabil* 2009; 90(12): 2146-54
26. Hills AP, Parker AW. Gait characteristics of obese children. *Arch Phys Med Rehabil* 1991; 72(6): 403-7

27. Adoracion Villarroya MA, Esquivel JM, Tomás C, Moreno LA, Buenafé A, Bueno G. Assessment of the medial longitudinal arch in children and adolescents with obesity: footprints and radiographic study. *Eur J Pediatr* 2009; 168(5): 559-67.
28. Van Boerum DH, Sangeorzan BJ Biomechanics and pathophysiology of flat foot. *Foot Ankle Clin* 2003; 8(3): 419-30
29. Hof AL. Scaling gait data to body size. *Gait Posture* 1996; 4: 222-3
30. Stansfield BW, Hillman SJ, Hazlewood ME, Lawson AA, Mann AM, Loudon IR, et al. Sagittal joint kinematics, moments, and powers are predominantly characterized by speed of progression, not age, in normal children. *J Pediatr Orthop* 2001; 21(3): 403-11

Figure 1 (a-d) All participant mean angular gait cycle waveform (solid line) with standard deviation (shaded area). (e-h) loading factors for rotated matrices determining contribution of gait cycle points to each component (horizontal line at .722 determined cut-off for part of gait cycle contributing to each PC). Vertical lines define the portion of the gait cycle captured in each component. (a, e) shank-calcaneus sagittal plane; (b, f) shank-calcaneus transverse plane; (c, g) calcaneus-midfoot sagittal plane; (d, h) calcaneus-midfoot frontal plane. Only significant results shown.

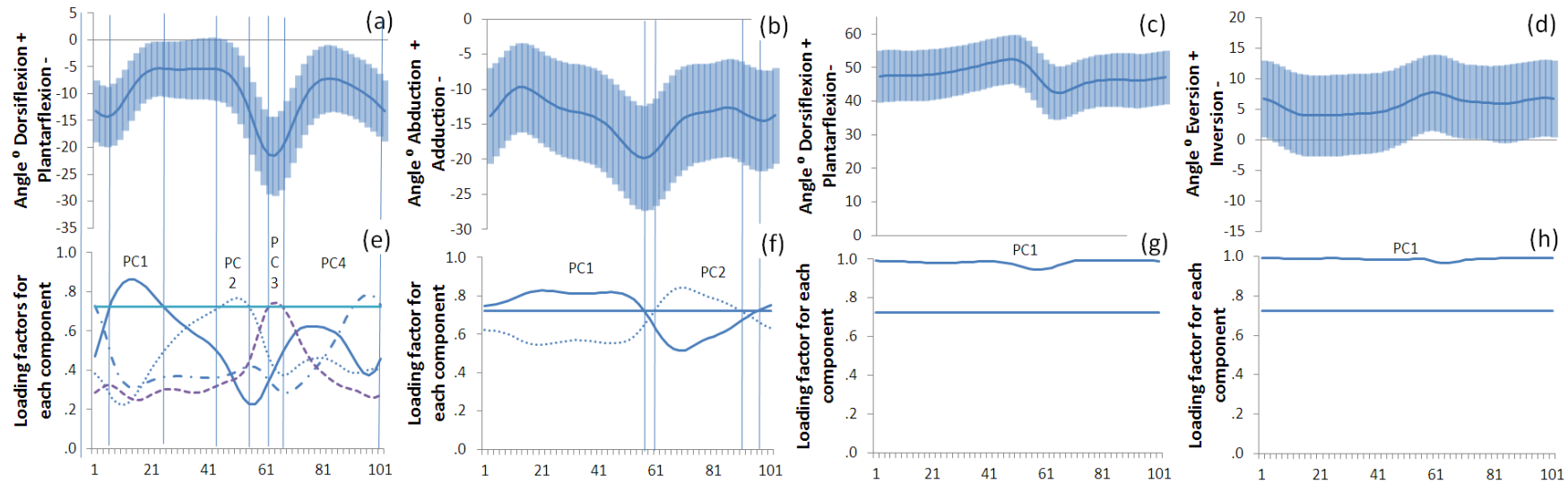


Figure 2. Representation of foot segment angular motion during gait associated with greater body fat.

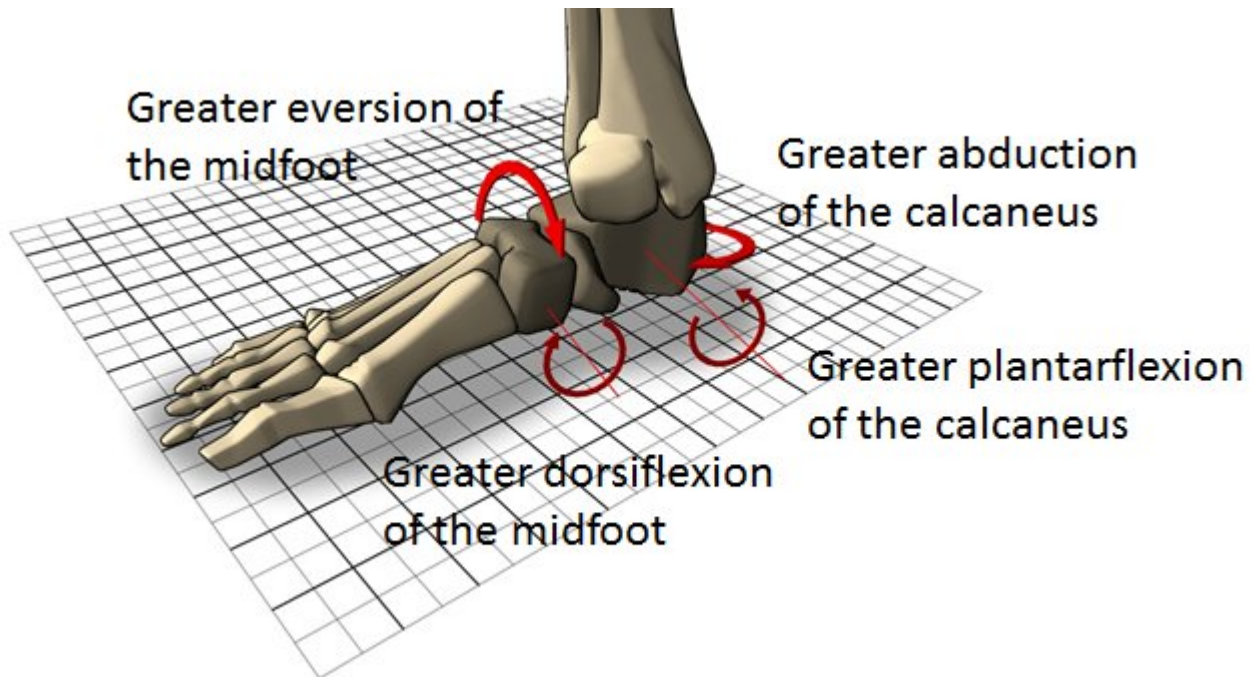




Table 1. Mean, SD and range of age, anthropometric and spatiotemporal characteristics of sample population (n=55)

|                                       | Mean   | SD    | Range           |
|---------------------------------------|--------|-------|-----------------|
| Age (years)                           | 9.55   | 1.18  | 7 - 11          |
| Height (m)                            | 1.40   | 0.08  | 1.19 – 1.59     |
| Weight (kg)                           | 37.69  | 10.67 | 22.3 – 68.6     |
| BMI (kg/m <sup>2</sup> )              | 18.41  | 4.00  | 12.34 - 29.62   |
| BMI Z-score                           | 0.55   | 1.58  | -2.87 - 3.54    |
| BMI Centile (%)                       | 59.99  | 36.08 | 0.21 - 99.98    |
| Body fat mass (%)                     | 23.78  | 9.33  | 9.46 – 42.06    |
| Walking velocity (m·s <sup>-1</sup> ) | 1.33   | 0.19  | 0.95 – 1.81     |
| Cadence (steps/min)                   | 131.69 | 15.66 | 105.77 – 171.52 |
| Stance Phase duration (%)             | 57.29  | 2.32  | 52.60 - 65.16   |
| Total single support duration (%)     | 49.86  | 1.85  | 41.59 – 56.70   |
| Step Width (mm)                       | 81.59  | 28.18 | 29.47 – 156.38  |
| Step length (m)                       | 0.60   | 0.06  | 0.41 – 0.79     |

Table2. Summary of principle component analysis of 3D foot segment angles. PC1 to PC4 represent the principle components extracted from each waveform. Only the parts of waveform that contributed to explain the variance in each component are shown

| Segment                              | Principle component  |                 |                      |                 |                      |                 |                      |                 |
|--------------------------------------|----------------------|-----------------|----------------------|-----------------|----------------------|-----------------|----------------------|-----------------|
|                                      | PC1                  |                 | PC2                  |                 | PC3                  |                 | PC4                  |                 |
|                                      | % Variance explained | % of gait cycle | % Variance explained | % of gait cycle | % Variance explained | % of gait cycle | % Variance explained | % of gait cycle |
| Shank-calcaneus: sagittal plane      | 33.94                | 7 to 25         | 25.51                | 45 to 55        | 21.99                | 93 to 1         | 16.19                | 63 to 65        |
| Shank-calcaneus: frontal plane       | 48.91                | 3 to 51         | 46.57                | 55 to 97        | -                    | -               | -                    | -               |
| Shank-calcaneus: transverse plane    | 53.01                | 99 to 55        | 43.78                | 61 to 89        | -                    | -               | -                    | -               |
| Calcaneus-midfoot: sagittal plane    | 96.56                | 0 to 100        | -                    | -               | -                    | -               | -                    | -               |
| Calcaneus-midfoot: frontal plane     | 97.39                | 0 to 100        | -                    | -               | -                    | -               | -                    | -               |
| Calcaneus-midfoot: transverse plane  | 99.31                | 0 to 100        | -                    | -               | -                    | -               | -                    | -               |
| Midfoot-metatarsal: sagittal plane   | 49.68                | 7 to 53         | 48.45                | 57 to 1         | -                    | -               | -                    | -               |
| Midfoot-metatarsal: frontal plane    | 96.97                | 0 to 100        | -                    | -               | -                    | -               | -                    | -               |
| Midfoot-metatarsal: transverse plane | 98.76                | 0 to 100        | -                    | -               | -                    | -               | -                    | -               |

Table 3. Summary of multiple regression analysis of regression score from PCA with predictor variables (only significant results are shown).

| Dependent variable                | Predictor variables $\beta$ (Std Error), $p$ value |                          |                              |                            |                          |                                 |   | Model $R^2$ | Model $p$ value |
|-----------------------------------|--|--------------------------|------------------------------|----------------------------|--------------------------|---------------------------------|---|-------------|-----------------|
|                                   | Body fat <sub>linear</sub>                         | Body fat <sub>quad</sub> | BMI ZScore <sub>linear</sub> | BMI ZScore <sub>quad</sub> | Height <sub>linear</sub> | Step distance <sub>linear</sub> | Stance phase duration <sub>linear</sub> |             |                 |
| Shank-Calcaneus: sagittal plane   |  |                          |                              |                            |                          |                                 |   |             |                 |
| PC1                               | -.04 (.02),<br>$p.009$                             | -                        | -                            | -                          | -                        | -                               | -.50 (.10),<br>$p.000$                  | .32         | .000            |
| PC2                               | -.03 (.02),<br>$p.046$                             | -                        | -                            | -                          | -                        | -                               | -                                       | .07         | .046            |
| PC3                               | -.04 (.02),<br>$p.022$                             | -                        | -                            | -                          | -                        | -                               | -                                       | .10         | .022            |
| Shank-Calcaneus: transverse plane |  |                          |                              |                            |                          |                                 |   |             |                 |
| PC1                               | .21 (.09),<br>$p.043$                              | .01 (.00),<br>$p.026$    | -                            | -                          | -                        | -                               | -                                       | .11         | .035            |
| PC2                               | .03 (.01),<br>$p.048$                              | -                        | -                            | -                          | -                        | -                               | -                                       | .07         | .048            |
| Calcaneus-Midfoot: sagittal plane |  |                          |                              |                            |                          |                                 |   |             |                 |
| PC1                               | .04 (.01),<br>$p.007$                              | -                        | -                            | -                          | -                        | -                               | -                                       | .13         | .007            |
| Calcaneus-Midfoot: frontal plane  |  |                          |                              |                            |                          |                                 |   |             |                 |
| PC1                               | .23 (.10),<br>$p.026$                              | .01 (.00),<br>$p.017$    | .38 (.13),<br>$p.007$        | .20 (.06),<br>$p.002$      | .06 (.02),<br>$p.003$    | .01 (.00),<br>$p.041$           | -                                       | .33         | .003            |